Korean Journal of Remote Sensing, Vol.26, No.3, 2010, pp.347~359

A New True Ortho-photo Generation Algorithm for High Resolution Satellite Imagery

Ki In Bang* and Changjae Kim** †

*Department of Geomatics Engineering, The University of Calgary

**School of Civil and Environmental Engineering, Yonsei University

Abstract : Ortho-photos provide valuable spatial and spectral information for various Geographic Information System (GIS) and mapping applications. The absence of relief displacement and the uniform scale in ortho-photos enable interested users to measure distances, compute areas, derive geographic locations, and quantify changes. Differential rectification has traditionally been used for ortho-photo generation. However, differential rectification produces serious problems (in the form of ghost images) when dealing with large scale imagery over urban areas. To avoid these artifacts, true ortho-photo generation techniques have been devised to remove ghost images through visibility analysis and occlusion detection. So far, the Z-buffer method has been one of the most popular methods for true ortho-photo generation. However, it is quite sensitive to the relationship between the cell size of the Digital Surface Model (DSM) and the Ground Sampling Distance (GSD) of the imaging sensor. Another critical issue of true ortho-photo generation using high resolution satellite imagery is the scan line search. In other words, the perspective center corresponding to each ground point should be identified since we are dealing with a line camera.

This paper introduces alternative methodology for true ortho-photo generation that circumvents the drawbacks of the Z-buffer technique and the existing scan line search methods. The experiments using real data are carried out while comparing the performance of the proposed and the existing methods through qualitative and quantitative evaluations and computational efficiency. The experimental analysis proved that the proposed method provided the best success ratio of the occlusion detection and had reasonable processing time compared to all other true ortho-photo generation methods tested in this paper.

Key Words : True Ortho-photo, High Resolution Satellite Imagery, Scan Line Search, Occlusion Detection.

1. Introduction

Ortho-photo production aims to eliminate sensor tilt and terrain relief effects from captured perspective imagery. Uniform scale and the absence of relief displacement make ortho-photos an important component of GIS databases. The users can directly determine geographic locations, measure distances, compute areas, and derive other useful information about the area in question using the ortho-photos. Recently, there has been a persistent need for an ortho-photo generation methodology that is capable

Received June 16, 2010; Revised June 18, 2010; Accepted June 21, 2010.

† Corresponding Author: Changjae Kim (earth2moon@gmail.com)

of dealing with the imagery acquired from high resolution satellite systems (e.g., IKONOS, OrbView, QuickBird, etc).

Ortho-photos are generated through a rectification procedure, which might be either forward or backward projection (Konecny, 1979; Novak, 1992). Forward projection procedure utilizes the available internal (or Interior Orientation Parameters, IOPs) and external characteristics (or Exterior Orientation Parameters, EOPs) of the imaging sensors to project the image contents onto the DSM cells. The DSM cell corresponding to the image pixel in question can be determined by intersecting a ray, which connects the perspective center and the image pixel, with the DSM. One should note that the EOPs of each scan line of the satellite imagery can be directly computed by using the trajectory model. Afterwards, DSM cell corresponding to each image pixel is found through an iterative procedure. One should note that the iterative procedure makes the computation load heavy (Chen and Lee, 1993). Moreover, the forward projection might leave some of the DSM cells with unassigned gray values. Therefore, a post-processing procedure is needed to interpolate the empty cells using the neighboring ones.

In contrast to the forward projection procedure, backward projection starts by projecting the DSM cell onto the image plane using the IOPs and EOPs. The gray value at the projected image location is acquired by interpolating the ones at neighbouring pixels. Finally, the interpolated gray value is assigned to the corresponding DSM cell. Fig. 1 shows the conceptual idea of ortho-photo generation through the backward projection procedure. The ground surface slope is not an issue in this method anymore. An iterative procedure for finding corresponding ground points is not required as well. Furthermore, all the DSM cells will have the assigned gray values. However, it does require a procedure for finding an

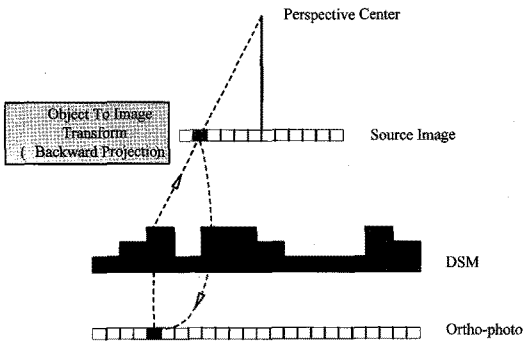

Fig. 1. Ortho-photo generation using backward projection procedure.

image pixel and its EOPs corresponding to the DSM cell in question because the external characteristics of each scan line change while an image is captured. This issue will be discussed in detail in the section where a proposed scan line search method is introduced.

Differential rectification is the commonly used term to denote a rectification of perspective imagery using backward projection procedure. It has been traditionally and widely used for ortho-photo generation. The performance of differential rectification procedure has been quite acceptable when dealing with medium resolution imagery over relatively smooth terrain. However, it produces significant artifacts in the form of ghost images (double mapped areas) at the vicinity of abrupt surface changes when we are dealing with high resolution imagery over urban areas (Skarlators, 1999; Habib, 2007). When we have two object points located on the same ray which is connecting these two object points, a corresponding image pixel, and the perspective center, the double mapped areas are caused by assigning the same gray value on these object points. Double mapped areas constitute a severe degradation of the interpretability of the generated ortho-photo. The effects of these artifacts can be mitigated by true ortho-photo generation methodologies which focus on the identification of occluded areas.

Hence, this paper will mainly focus on two issues: scan line search and occlusion detection in the procedures of the true ortho-photo generation. Section 2 will discuss the proposed scan line search method while comparing the shortcomings of the existing ones. Afterwards, the existing occlusion detection and true ortho-photo generation methods (which are widely used ones) and its variants will be described in Section 3 to handle the second issue. Newly proposed true ortho-photo generation method which overcomes the shortcomings of the existing ones will be explained in Section 4. Then, experimental results and analysis will be presented in Section 5. Finally, conclusions and recommendations for future work are summarized.

2. Iterative Scan Line Search Method

One should note that the EOPs of each scan line that makes up the scene are not the same because the scanner continually moves along its trajectory during data acquisition. Hence, knowing when the sensor captured a particular object point is critically important, especially, when we are dealing with line scanner images to generate true ortho-photos through differential rectification procedure. Chen and Lee (1993) used Newton Raphson method to solve a non-linear equation which includes positional and attitude parameters of satellite imaging system. However, this method is carried out numerically and is very sensitive to the initial value (Kincaid and Cheney, 1996; Kim *et al.*, 2001). Hence, Kim *et al.* (2001) proposed *Back-Tracing algorithm* to overcome the limitations of *Chen and Lee's algorithm*. Even though *Back-Tracing algorithm* solved the problems of *Chen and Lee's algorithm*, it has its own limitation, that it has a part to solve non-linear equation when the imaging time of a particular scan line is updated. This part needs to be solved either by an iterative procedure after linearization or a numerical method. Recently, Wang *et al.* (2009) proposed another approach based on the assumption of parallel perspective plane of scan-line and constant speed of imaging craft. Since their method is based on such assumptions, it might not be applicable to real situation where we have an imaging system with non-constant flying speed and perturbation in its trajectory.

A scan line search method proposed (named *Iterative Scan Line Search Method*) in this paper is designed to be simple and to overcome the limitations of the previous scan line search algorithms. In other words, the proposed algorithm does not include numerical computation and linearization procedure. Moreover, it aims at handling all possible realistic trajectory models regardless of their mathematical complexity (e.g., degree of a polynomial).

The well-known collinearity equations for line scanner images are described as follows:

$$x = -f\frac{m_{t11}(X-X_t)+m_{t12}(Y-Y_t)+m_{t13}(Z-Z_t)}{m_{t31}(X-X_t)+m_{t32}(Y-Y_t)+m_{t33}(Z-Z_t)}$$
$$y = -f\frac{m_{t21}(X-X_t)+m_{t22}(Y-Y_t)+m_{t23}(Z-Z_t)}{m_{t31}(X-X_t)+m_{t32}(Y-Y_t)+m_{t33}(Z-Z_t)} = d \quad (1)$$

Where

(x,y)	are the image coordinates of an object,
(X,Y,Z)	are the ground coordinates of an object point,
d	is the offset value for the line scanner in the y-direction,
f	is the focal length of the lens,
(X_t,Y_t,Z_t)	are the ground coordinates of the perspective center at time t,
$mt_{11}\cdots mt_{33}$	are the elements of the rotation matrix at time t.

The perspective center corresponding to an object point in question can be found through an iterative procedure using the properties of a one dimensional image. More specifically, any scan line can be chosen arbitrarily for an initial location and attitude of the

perspective center; for example it should be fine to select a scan line located at the middle of the whole image. Afterwards, the image coordinates are calculated using the coordinates of the object in question, and the initial location and attitude of the perspective center in Equation 1. Since the used location and attitude of the perspective center are approximate we expect that there might be a discrepancy between the calculated y image coordinate (along the flight direction) and d (i.e., the offset value for the line scanner) (Fig. 2a). The discrepancy in the y coordinate can be used to update the initial location and attitude of the perspective center. The updated time of the perspective center can be computed by using Equation 2. The steps abovementioned repeat until the discrepancy is lower than a pre-defined threshold (e.g., half of the image pixel size). Fig. 2b illustrates the conceptual idea of the proposed *Iterative Scan Line Search Method*. Once we have the solution of the location and attitude of the perspective center in question, an image pixel corresponding to the respective object point can be finally determined. To improve the efficiency of the computation, the initial values of the perspective center corresponding to the object point in question can take the adjacent DSM cell's solution of the perspective center if the solution exists.

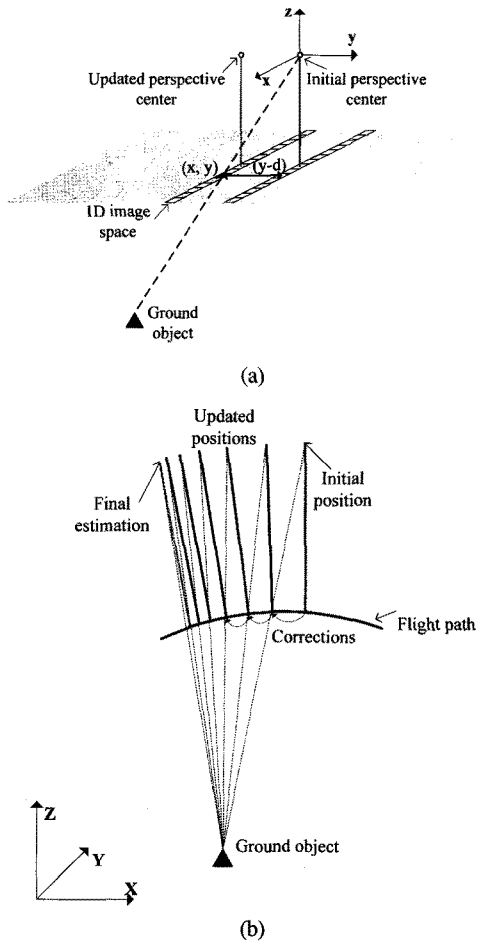

Fig. 2. The Iterative Scan Line Search Method: discrepancy between the expected and calculated y coordinate is used for updating the initial EOPs (a), and the iterative search procedure stops when the discrepancy is less than the pre-defined threshold (b).

$$t_{n+1} = t_n + \frac{y - d}{\Delta L} \qquad (2)$$

Where:

ΔL is the scanning rate,
t_n is the approximate scanning time,
t_{n+1} is the updated scanning time, and
$(y - d)$ is the discrepancy.

3. Existing True Ortho-photo Generation Methodologies and Their Limitations

Once we have correct location and attitude of the perspective center corresponding to an object point in question, next step will be true ortho-photo generation while mainly focusing on the identification of occluded areas. Kuzmin *et al.* (2004) and Zhou *et al.* (2005) proposed true ortho-photo generation methods based on a Digital Building Model (DBM) for airborne large scale frame imagery. In these methods, conventional digital differential rectification is first applied. Afterwards, hidden areas are detected through the use of

polygonal surfaces generated from a DBM. With the exception of the methodologies using a DBM, the majority of existing true ortho-photo generation techniques using a DSM is based on the *Z-buffer method* (Catmull, 1974; Amhar *et al.*, 1998; Rau *et al.*, 2000; Rau *et al.*, 2002; Sheng *et al.*, 2003). The Z-buffer algorithm proposed by Amhar *et al.* (1998) has mainly been used for true ortho-photo generation. As can be seen in Fig. 3, double mapped areas arise from the fact that two object space points (e.g., A and D, B and E, or C and F) are competing for the same image location (e.g., d, e, or f, respectively). The Z-buffer method resolves the ambiguity regarding which object point should be assigned to a certain image location by considering the distances between the perspective center and object points in question. Among the competing object points, the points (e.g., D, E, and F) closest to the perspective center of an image is considered to be visible, while the other points (e.g., A, B, C) are considered to be invisible in that image. Finally, the visible points will have the corresponding gray values (e.g., g(d), g(e), or g(f)) from the image space; however, the invisible ones will have black values.

Using the common properties of the satellite images, we can simply modify the original Z-buffer method more efficiently. As mentioned previously, the distances from the objects to the perspective center are utilized to determine the visibility of each DSM cell in the original Z-buffer method. In this regard, the distances and the coordinates of the DSM cells are recorded in the additional memory space (so called Z-buffer array). At this stage, it is worth noting that satellite images are captured by imaging sensors above the object space; therefore, higher points on the object space are closer to the perspective center than lower points. For this reason, the elevations of DSM cells can be directly used in the visibility analysis procedure instead of distances between the object points and corresponding perspective centers. This modification leads to less computational load compared to the original Z-buffer method. In the same line of thought, the DSM cells which are sorted according to their height values can be used for the visibility analysis (or occlusion detection). This will remove the necessity of recording the elevations of DSM cells in the additional memory space (i.e., Z-buffer array). More specifically, the visibility analysis will start from the highest DSM cell to the lowest one. The DSM cell in question will be first projected onto the image space. Then, the gray value of the corresponding image pixel will be assigned to the DSM cell. Afterward, the original gray value of the image pixel will be changed to black. This will prevent the projection of the same gray value more than once. In other words, the visible DSM cells will have the original gray values of the image space and the invisible ones will always have black values. This method will be referred to henceforth as the *Sorted DSM method*. The computational load of this method strongly depends upon the sorting algorithm used because sorting procedure is computationally heavy and complex. Nevertheless, once one already has a sorted DSM, this method will provide a benefit since

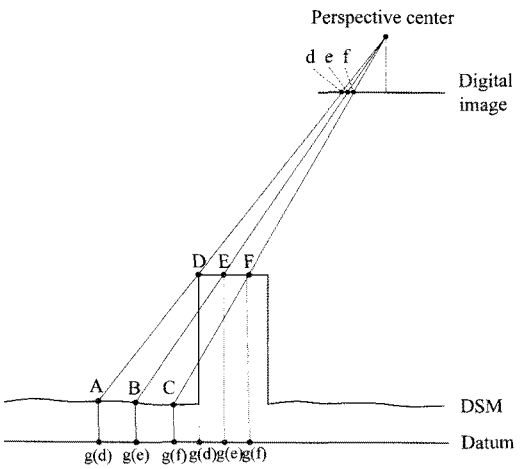

Fig. 3. Concept of Z-buffer method.

the memory space for Z-buffer array is not necessary anymore.

At this stage, one should note that the Z-buffer method and its variants (which are based on the same idea as the Z-buffer method) has several limitations. More specifically, such methods suffer from several problems such as the sensitivity to the sampling interval of the DSM, as it relates to the ground sampling distance (GSD) of the imaging sensor. Moreover, they provide true ortho-photos with false visibility associated with narrow vertical structures. This problem is commonly known in the photogrammetric literatures as the M-portion problem, which can be resolved by introducing additional artificial points (pseudo ground points) along building facades (Rau *et al.*, 2000; 2002). The Z-buffer method after introducing pseudo ground points is called the *Modified Z-buffer method* in this paper. The modified Z-buffer method alleviates the M-portion problem of the Z-buffer method; however, it has heavy computational loads caused by the introduced pseudo ground points and still can not avoid the abovementioned sensitivity problem perfectly. For more details regarding the drawbacks of the Z-buffer method and modified Z-buffer method, interested readers can refer to Habib *et al.* (2007).

4. Proposed True Ortho-photo Generation Method (Height Based Ray Tracing Method)

This research proposes a new occlusion detection method to overcome the significant drawbacks of the existing true ortho-photo generation methods which are discussed in the previous section. The basic principle of the proposed method (hereafter this will be called *Height Based Ray Tracing method*) is that, if a certain object point has been successfully captured by the cameras or scanners, then there is no point which intercepts the projection ray, which connects the object and the corresponding perspective center. More specifically, we will check whether any object point located on the search path, which is the footprint of the projection ray onto the object space, is higher than the projection ray (refer to Fig. 4). For example, in the figure, the object point in question (i.e., object 0) will be identified as an invisible point since the object point 2 is higher than the projection ray. Once the visibility analysis has been completed, the corresponding gray values will be assigned onto the visible points only.

The implementation of the Height Based Ray Tracing method for occlusion detection and true ortho-photo generation can proceed according to the following steps (refer to the procedures in Fig. 5 as well):

1. An object point (or a DSM cell) in question is selected as a target point.
2. The corresponding perspective center of the point can be determined by using the Iterative Scan Line Search method explained in Section 2.
3. A projection ray is determined by using the three

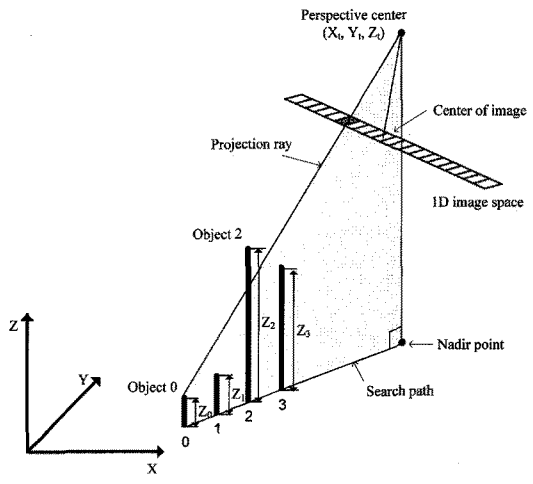

Fig. 4. Basic concept of Height based ray tracing method.

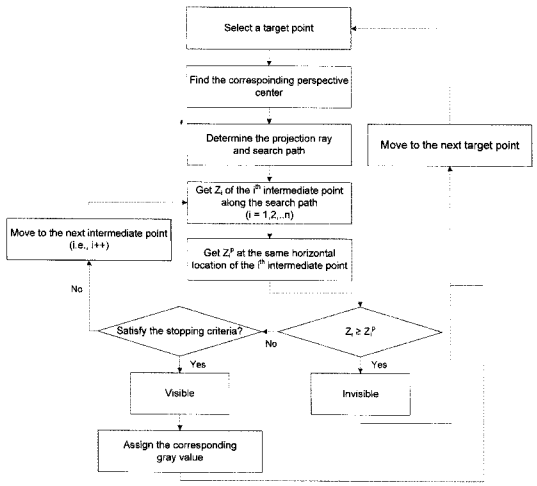

Fig. 5. The procedures of the Height Based Ray Tracing method.

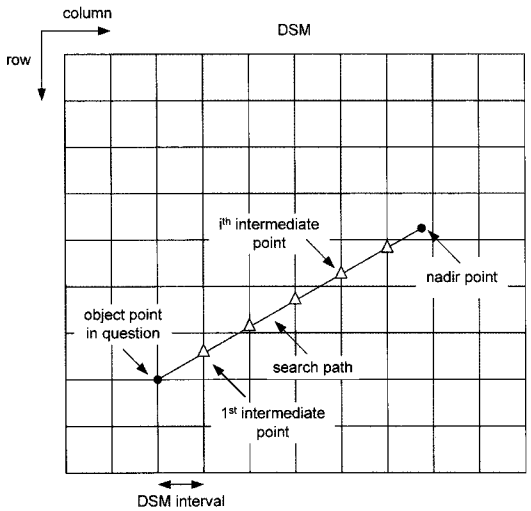

Fig. 6. Intermediate points along the search path for the object point in question.

dimensional coordinates of the target point and the corresponding perspective center.

4. A search path is defined by the projection of the target point onto the datum and the corresponding nadir point of the perspective center. In other words, the search path is determined using the horizontal coordinates of the target point and the perspective center.
5. The horizontal coordinates of intermediate points located along the search path can be determined while considering the DSM interval and the slope of the search path. The vertical coordinates (or heights) of the intermediate points will be calculated through bi-linear interpolation using four neighboring DSM cells (Fig. 6).
6. Once the first intermediate point, which is the closest point to the target point along the search path, is selected, the height of the intermediate point (i.e, Z_i) and that of the projection ray (i.e., Z_i^p) at the same horizontal location of the intermediate point are compared to each other.
7. The target point will be identified as an invisible point if the height of the intermediate point is higher than that of the projection ray (i.e., $Z_i \geq Z_i^p$). Otherwise, we will check whether one of the stopping criteria is satisfied. Three stopping criteria: 1) the height of the projection ray is higher than the maximum value of the given DSM; 2) the horizontal position of the intermediate point reaches the nadir point of the perspective center; 3) the horizontal position of the intermediate point reaches the boundary of the DSM, will be considered.
8. If one of the stopping criteria mentioned in Step 7 is satisfied, the target point will be identified as a visible point. The gray value for the visible point will be imported from the original image. When the stopping criteria are not satisfied, we move to the next intermediate point along the search path and repeat Step 7 to 8.
9. One should note that all the steps from 1 to 8 are for a single target point. Hence, we will move to the next target point once the visibility analysis and the assignment of the gray value for the current target point have been completed.

Unlike Z-buffer method and its variants, the resolution of the original image is not an issue in the Height Based Ray Tracing method because only the

ground points and the corresponding perspective centers are used to search for the occlusion areas. Therefore, the proposed true ortho-photo generation method will produce more correct and clear boundaries and occlusion areas when compared to the Z-buffer method and its variants. More detailed analysis of the proposed method will be addressed in the next section while comparing with the existing true ortho-photo generation methods.

5. Experimental Results and Analysis

To verify the performance of the developed true ortho-photo generation method, several experiments using real data were conducted. Five methods for generating true ortho-photos: 1) Conventional differential rectification; 2) Z-buffer method; 3) Sorted DSM method; 4) Modified Z-buffer method; and 5) Height based ray tracing method, are tested and compared to each other in this section. Qualitative and quantitative evaluations of such different methods are carried out by comparing the true ortho-photos produced.

The real data is comprised of IKONOS stereo satellite images and a LiDAR surface model over the City of Daejeon, South Korea. The exterior and interior orientation parameters of the imaging sensor are also available. The DSM derived from LiDAR data has 1.0 m resolution, and the satellite images have about 1.0 m nominal resolution. Figs. 7a and 7b show the DSM and the IKONOS image over the area of interest, respectively. To carry out the qualitative evaluation of the products from the different true ortho-photo generation methods, one sample area is selected and enlarged from the original satellite image and the generated true ortho-photos as shown in Fig. 8.

As can be seen in Fig. 8a the original satellite image has relief displacements which cause occlusions. The conventional differential rectification method is used to get rid of the relief displacements, which are shown in the original satellite image. However, it produces the double mapped areas caused by occlusions where we have abrupt surface changes as shown in Fig. 8b. To avoid this double mapping problem, Z-buffer method, Sorted DSM method, Modified Z-buffer method, and Height based ray tracing method are used to remove the double mapped areas and to fill with black color instead of the original image textures as shown in Figs. 8c, 8d,

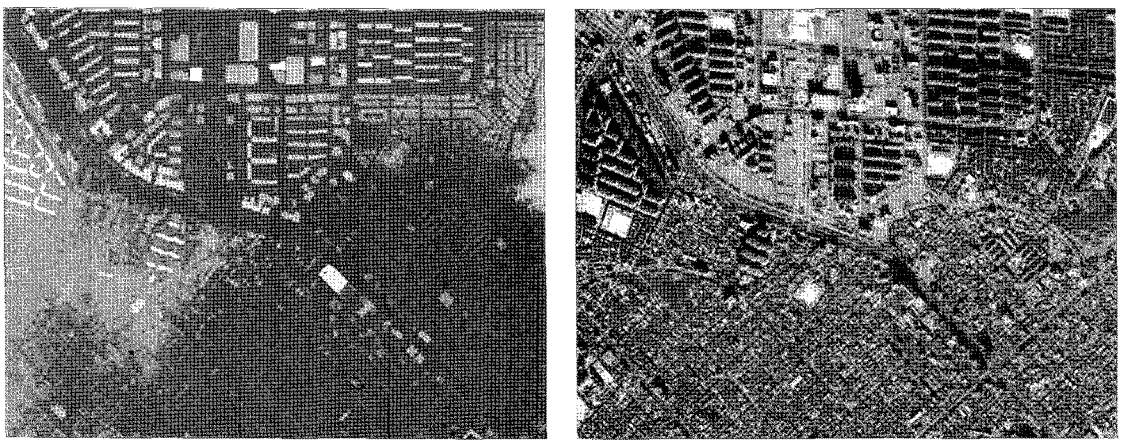

(a) (b)

Fig. 7. The LiDAR DSM (a) and the IKONOS image (b) over the City of Daejeon, South Korea.

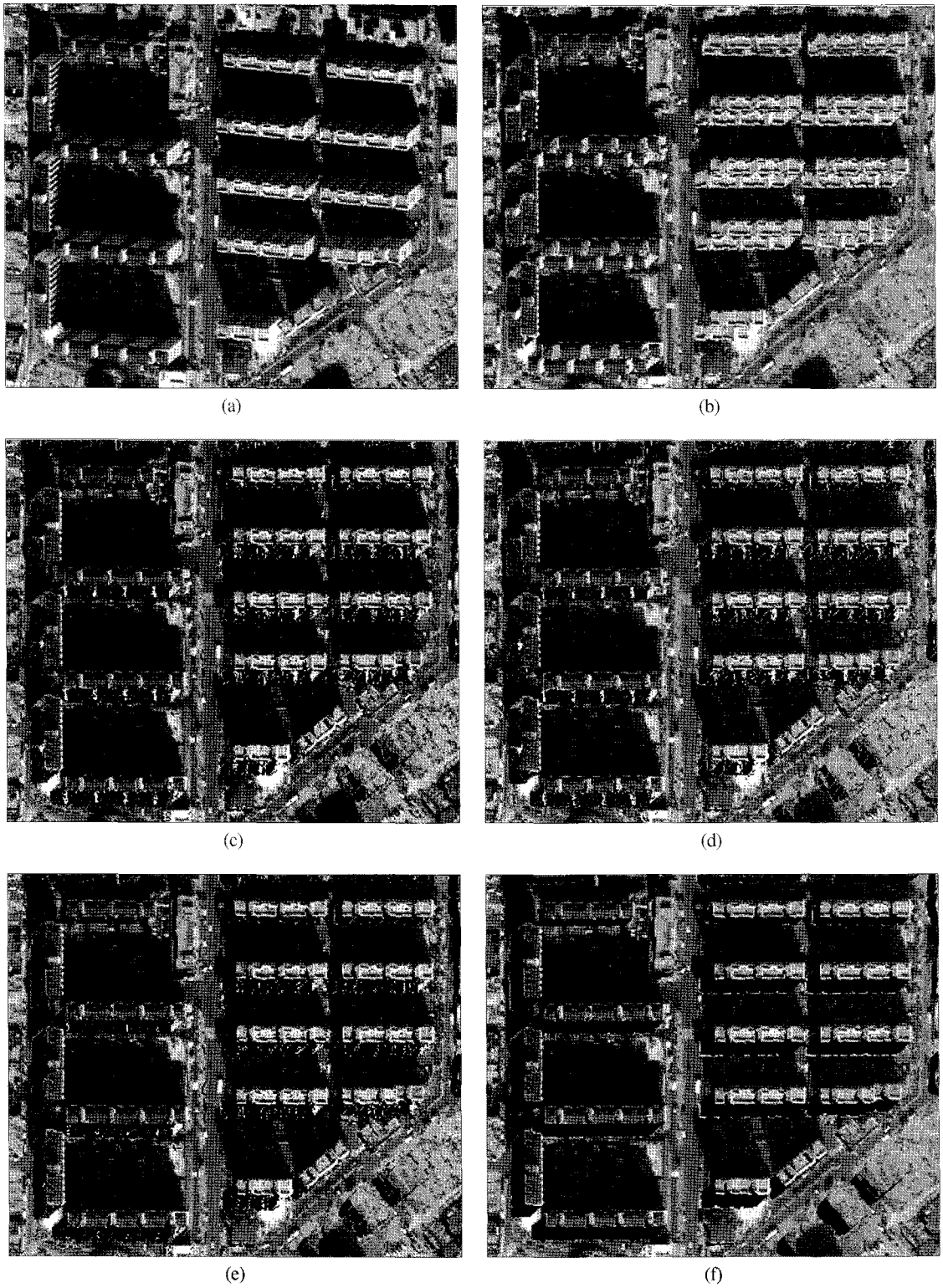

(a) (b)

(c) (d)

(e) (f)

Fig. 8. Original satellite image (a), different true ortho-photos generated by the conventional differential rectification method (b), Z-buffer method (c), Sorted DSM method (d), Modified Z-buffer method (e), and Height based ray tracing method (f).

8e, and 8f, respectively. The quality of the true ortho-photo produced by Z-buffer method (in Fig. 8c) is pretty similar to that produced by Sorted DSM method (in Fig. 8d). One can visually check that these two figures have significant false visibility in the occlusion areas. The Modified Z-buffer method shows better quality compared to the Z-buffer and the Sorted DSM method in the occlusion areas as shown in Fig. 8e. Nevertheless, the true ortho-photo produced by the Modified Z-buffer method still has false visibility. The Height based ray tracing method proposed in this study provides better result than other methods in terms of false visibility in the occlusion areas (refer to Fig. 8f).

This part of the experimental results provides a quantitative evaluation of the Height based ray tracing method, while comparing with the other methods. To statistically check the performances of the different true ortho-photo generation methods, fifteen polygons enclosing occlusion areas are, first, measured manually in the ortho-photo generated by the conventional differential rectification method. A sample of polygon with red color is projected onto the true ortho-photos generated by different methods as shown in Fig. 9.

A statistical measure defined as Equation 3 is used to evaluate the success ratio of detecting occlusion areas for each true ortho-photo generation method. Table 1 shows total number of correctly detected occlusion pixels in the polygons, total number of pixels in the polygons, and the calculated success ratio of the occlusion detection for each true ortho-photo generation method. As can be seen, Height based ray tracing method has the best success ratio (i.e., 94.04%) compared to other methods. About 6% of the failure in the occlusion detection evaluation is mostly caused by the pixels located on the polygon boundaries (i.e., red lines in Fig. 9). The main reason for this failure is that the noises from the geo-referencing results and the interpolated DSM mostly affect where there are sudden changes of elevations (e.g., like the building boundaries), which are mostly corresponding to the polygon boundaries (i.e., red lines in Fig. 9). One should note that the reason for the failure of the occlusion detection on (or near) the polygon boundaries is common to all other methods tested in this paper as long as we are dealing with the same satellite images and DSM. Hence, the differences of the success ratios shown in Table 1 mostly come from the different performances of the true ortho-photo generation methods, which are about how well the methods can detect occlusions inside the polygons.

$$\text{Success ratio} = \frac{\text{Total number of correctly detected occlusion pixels in the polygons}}{\text{Total number of pixels in the polygons}} \quad (3)$$

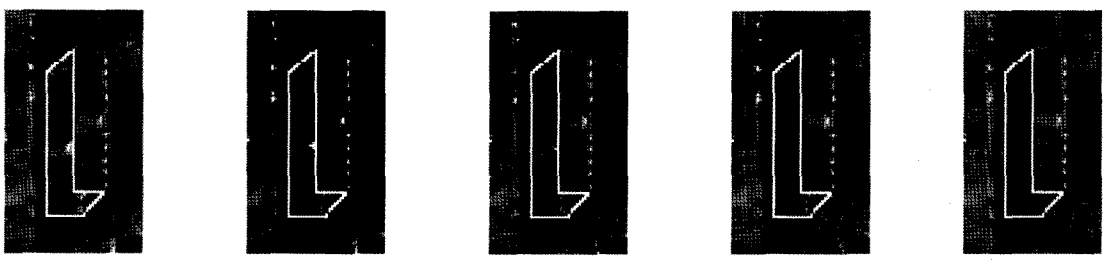

(a) (b) (c) (d) (e)

Fig. 9. A sample polygon projected onto the true ortho-photos generated by five different methods: the conventional differential rectification method (a), Z-buffer method (b), Sorted DSM method (c), Modified Z-buffer method (d), and Height based ray tracing method (e).

Table 1. Success ratios of the occlusion detection for five different true ortho-photo generation methods

True ortho-photo generation method	Total number of correctly detected occlusion pixels in the polygons	Total number of pixels in the polygons	Success ratio (%)
Differential rectification	0	8847	0
Z-buffer	6533	8847	73.84
Sorted DSM	6520	8847	73.70
Modified Z-buffer	7672	8847	86.72
Height based ray tracing	8320	8847	94.04

More than the success ratio of the occlusion detection, we compared the processing times of the five true ortho-photo generation methods in Fig. 10. The differential rectification method is the fastest method and the Modified Z-buffer method is the slowest one. Except for the Modified Z-buffer method, the elapsed times of all other methods are different less than around 10sec.

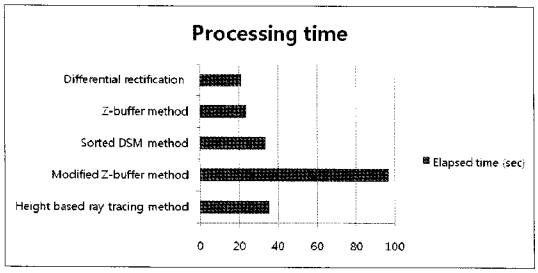

Testing conditions:
- CPU: Athlon 2.6 GHz, and Memory: 1,024 MB
- Data size: Image 13816 X 13824, and DSM 1449 X 1692

Fig. 10. Processing time of the tested methods.

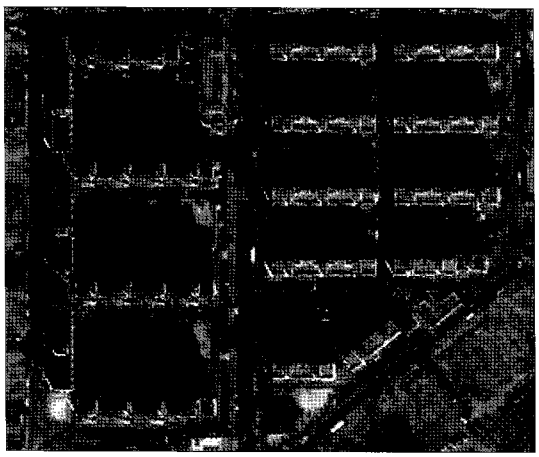

Fig. 11. Occlusion recovery result using multiple images after producing the true ortho-photos by the Height based ray tracing method.

For the improved visual quality, the missing information in the detected occlusion areas in a true ortho-photo is recovered by the merging of multiple images. In other words, the occlusion areas with no texture information can be filled with other texture information from the images which were taken at the different positions. In this regard, Fig. 11 shows the occlusion recovery result using multiple images after producing the true ortho-photos by the Height based ray tracing method.

6. Conclusions

True ortho-photo generation faces a challenge with line scanner images that it does not face with frame images, because line scanners continually move during image capturing, and each scan line has its own location and attitude of the perspective center. For this reason, we had to consider two technical issues in generating true ortho-photos; these are: 1) scan line search, and 2) occlusion detection for the multiple exposure centers. To resolve the first issue, a novel and computationally simple scan line search method, *Iterative Scan Line Search Method*, is proposed in this paper. It does not have numerical computation and linearization procedure, which might be shortcomings of the existing scan line search method. Moreover, it is designed to handle all

possible realistic trajectory models. To deal with the second issue, the performances of the proposed *Height Based Ray Tracing Method*, and the four existing ones are compared qualitatively and quantitatively. Height based ray tracing method had practically reasonable processing time and showed about 94% of the success ratio in the occlusion detection evaluation, which is the best result compared to the other methods. Through the experimental results and analysis, we proved that the proposed scan line search and occlusion detection methods would be feasible, robust, and practical alternatives for true ortho-photo generation compared with other methods.

For the future work, the noise effect from the geo-referencing results and the interpolated DSM on the occlusion detection performance (which caused around 6% of the failure in the occlusion detection evaluation) will be considered and might be mitigated by expanding the detected occlusion areas.

References

Amhar, F., J. Jansa, and C. Ries, 1998. The generation of true orthophotos using a 3D building model in conjunction with a conventional DTM, International Archives of Photogrammetry and Remote Sensing, 32(Part 4): 16-22.

Catmull, E., 1974. A Subdivision Algorithm for Computer Display of Curved Surfaces, Ph.D. dissertation, Department of Computer Science, University of Utah, Salt lake city, Utah.

Chen, L., and L. Lee, 1993. Rigorous generation of digital orthophotos from SPOT images, Photogrammetric Engineering and Remote Sensing, 59(5): 655-661.

Habib, A., E. Kim, and C. Kim, 2007. New methodologies for true ortho-photo generation, Photogrammetric Engineering and Remote Sensing, 73(1): 025-036.

Kincaid, D., and W. Cheney, 1996. Numerical Analysis: Mathematics of Scientific computing, Second Edition, Brooks/Cole, Pacific Grove, California, 804 p.

Kim, T., D. Shin, and Y. Lee, 2001. Development of a robust algorithm for transformation of a 3D object point onto a 2D image point for linear pushbroom imagery, Photogrammetric Engineering and Remote Sensing, 67(4): 449-452.

Konecny, G., 1979. Methods and possibilities for digital differential rectification. Photogrammetric Engineering & Remote Sensing, 45(6): 727-734.

Kuzmin, P., A. Korytnik, and O. Long, 2004. Polygon-based true orthophoto generation, XXth ISPRS Congress, 12-23 July, Istanbul, pp. 529-531.

Novak, K., 1992. Rectification of digital imagery, Photogrammetric Engineering and Remote Sensing, 58(3): 339-344.

Rau, J., N. Chen, and L. Chen, 2000. Hidden compensation and shadow enhancement for true orthophoto Generation, Proceedings of Asian Conference on Remote Sensing 2000, 4-8 December, Taipei, unpaginated CD-ROM.

Rau, J., N. Chen, and L. Chen, 2002. True orthophoto generation of built-up areas using multi-view images, Photogrammetric Engineering and Remote Sensing, 68(6): 581-588.

Sheng, Y., P. Gong, and G. Biging, 2003. True orthoimage production for forested areas from large-scale aerial photographs, Photogrammetric Engineering and Remote Sensing, 69(3): 259-266.

Skarlatos, D., 1999. Orthophotograph production in urban Areas, Photogrammetric Record, 16(94): 643-650.

Wang, E., F. Hu, J. Li, and J. Pan, 2009. A fast approach to best scanline search of airborne linear pushbroom images, Photogrammetric Engineering and Remote Sensing, 75(9): 1059-1067.

Zhou, G., W. Chen, J. A. Kelmelis, and D. Zhang, 2005. A Comprehensive Study on Urban True Orthorectification, IEEE Tansactions on Geoscience and Remote Sensing, 43(9): 2138-2147.